

Electric Field and SAR Distribution in the Vicinity of Orthodontic Brace Exposed to the Cell Phone Radiation

Dejan B. Jovanovic¹, Dragan Dj. Krasic², Vladimir B. Stankovic³, Nenad N. Cvetkovic¹, and Dragan D. Vuckovic¹

¹ Faculty of Electronic Engineering
University of Nis, Nis, 18000, Serbia
dejan.jovanovic@elfak.ni.ac.rs, nenad.cvetkovic@elfak.ni.ac.rs, dragan.vuckovic@elfak.ni.ac.rs

² Faculty of Medicine
University of Nis, Nis, 18000, Serbia
dragan.krasic@medfak.ni.ac.rs

³ Faculty of Occupational Safety
University of Nis, Nis, 18000, Serbia
vladimir.stankovic@znrak.ni.ac.rs

Abstract — The aim of this study is to investigate the impact of orthodontic brace on the electric field distribution and amount of the absorbed energy from the cell phone within the teeth. A comparative analysis of the models (child and adult) with and without brace has been carried out due to different morphological and tissue characteristics of child's and adult's head. The 3D realistic models of the child's and adult's head, with the jaw having the orthodontic brace, have been designed. The shapes and features of the child and adult head model, as well as the distance between the electromagnetic source and the exposed object, have an important role in the evaluation of the Specific Absorption Rate (SAR). The applied procedure is based on the numerical solution of the electromagnetic waves propagation equations. The numerical analysis has been performed at the frequency of 3G (0.9GHz). The obtained results are represented within the teeth positioned on the side of the electromagnetic radiation source. Based on the obtained results, one can conclude that the presence of orthodontic brace affects the increase of electric field and SAR within the teeth.

Index Terms— Adult's head model, cellphone, child's head model, electric field distribution, orthodontic braces, specific absorption rate.

I. INTRODUCTION

Orthodontic treatment deals with the correction of inborn and gained anomalies in teeth position. That includes using dental braces in order to ensure alignment in a natural way by the movement of the teeth. The main goal of dental braces usage is to provide the proper

function of teeth and to improve dental health. There are different types of aesthetic brace systems as well as the different materials for producing the orthodontic braces. Most commonly, metal wires are inserted into orthodontic braces made from stainless steel.

According to previous studies, one can find that the metal objects can significantly increase the amount of absorbed energy. The authors in [1] have found that the SAR values can be several times greater in the presence of metal object. The effect of electromagnetic radiation from mobile phone on nickel release from orthodontic brackets has been taken into consideration in study [2]. It is found that the concentration of nickel in the artificial saliva in the exposure group was significantly higher than that of the control group. The level of the nickel released in this investigation was far below the toxic level but maybe enough that can lead to allergic reaction in humans. One of the previously studies [3] reported the involuntary movements of the subjects, which had gold (metal) alloy dental inlay, caused by electromagnetic waves.

As it is well known, cell phones and communication systems have been developed at an astounding rate. This brings significantly increased exposure to electromagnetic (EM) cell phone radiation, which turned the focus towards researching of the impact of electromagnetic waves on human organism and estimation of human health risk.

Despite the concerns about the health effects of long-term exposure to RF radiation, the popularity of wireless devices among the children is growing rapidly. Today's children will certainly have much more exposure to cell phone radiation than adults [4].

The safety measures that prescribe the maximum allowable levels for exposure to electromagnetic fields have been adopted in safety standards [5-8]. Moreover, the electromagnetic field has been characterized as potentially carcinogenic to humans and classified as a group 2B carcinogen [9].

Numerous studies, which refer to the impact of the electromagnetic radiation from the cell phones, deal with the numerical analysis of electric field and SAR distribution within the biological tissues inside the human head [10-17], but not in the oral region.

The main aim of this study is to determine the orthodontic brace impact on the electric field distribution and SAR values inside the certain teeth, while using the cell phone. Moreover, these results take into account the age of the cell phone user. Therefore, the paper deals with the comparative analysis of these results when orthodontic braces are embedded in child's and adult's head model.

Hence, numerical analysis of electric field distribution, as well as values of the absorbed energy in the vicinity of an orthodontic brace (metal object positioned at the surface of teeth), has been performed and presented in this paper. For this purpose, the actual smartphone, as a source of EMF radiation, has been modeled for this study.

The shapes of the head model, its features and the distance between the electromagnetic source and the exposed object, have an important role in the evaluation of the amount of the absorbed electromagnetic energy. The numerical calculations of the electric field and SAR values have been performed by using the Computer Simulation Technology (CST) software package [18]. Numerical analysis has been performed at the frequency of 3G mobile network $\sim 0.9\text{GHz}$.

II. METHOD AND MODELING

A. Model

In order to determine the electric field and SAR distribution in the vicinity of orthodontic brace exposed to the cell phone radiation, the 3D realistic models of the child's and adult's head as well as the jaw with the orthodontic brace have been developed. In addition to the essential differences in size and shape of the head of adults and child [4, 19-26], the differences in morphology and composition of tissues are also included as parameters in this investigation (Fig. 1, Table 1 and Table 2). This primarily refers to the amount of water content in tissues, and the growth of various organs with age [27]. Anatomical and morphological characteristics of head models correspond to the seven year old child and an average adult person (Fig. 1). Both models (child and adult) have the same construction, consisting of the following tissues and biological organs: Cortical Bones, Brain, Cerebrospinal Fluid, Fat, Cartilage, Pituitary Gland, Spinal Cord, Muscle, Eyes, Skin, Tongue and

Teeth. The cross-section of the 3D realistic child's and adult's head model with biological tissues and organs is shown in Fig. 1.

The whole process of head models design was performed in few stages. First, it is necessary to design the external looks of the biological organs and tissues, whose shape replicates the actual human head appearance. Then, they are used as a base for creating the head models for numerical analysis. Also, during the process of creating the head models, it is important that the biological organs are modelled such that they don't overlap each other. In this way, it is possible to consider the boundary conditions at the separation area between two tissues during the propagation of EM waves from one tissue into another.

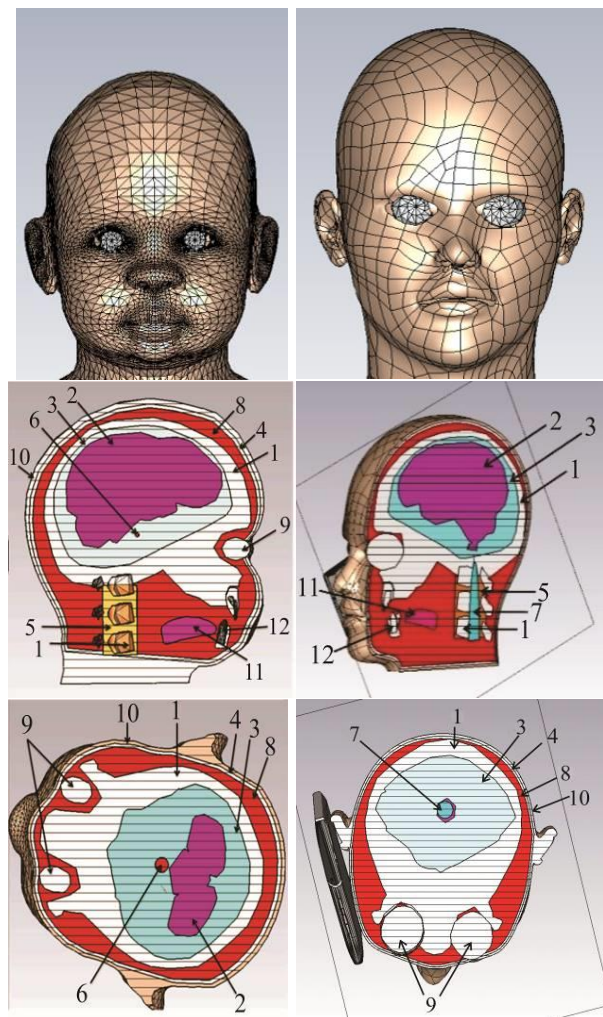


Fig. 1. External appearance and cross-section of the child's head model (left) and adult's head model (right).

The detailed knowledge of the electromagnetic properties (permittivity, conductivity and density) is necessary in order to understand the interaction between

electromagnetic radiation and the exposed object. The effects of propagation, reflection and attenuation of electromagnetic waves within the human body depend on the electromagnetic properties of biological tissues and organs. These parameters are highly dependent on the tissue type and the frequency.

Also, the age dependence of dielectric properties of biological tissues mainly relies on the fact that the permittivity and electrical conductivity can be expressed as a function of water content in the tissue.

The concentration of the water varies depending on the age of tissue. As the content of the water in the tissue increases, the conductivity equally increases. As the frequency increases, the conductivity also increases, but the permittivity decreases. It should be noted that the relative magnetic permeability is assumed to be 1.

The values of electromagnetic properties for an adult person and a child [27-31], for the above mentioned frequencies, are shown in Table 1 and Table 2 respectively. Numerical designations for electromagnetic properties for tissues and organs from Tables correspond to those from Fig. 1.

In addition, the most frequently used material for orthodontic brace is the stainless steel (FeCrNi), containing 18–20% of chromium and 8–10% of nickel [32], due to the stainless steel with the electrical resistivity $\rho=7.2 \times 10^{-7} \Omega\text{m}$, which has been used in simulation.

In order to obtain the most accurate results, the assembled model (orthodontic brace model and jaw model) shown in Fig. 2 (b), has been designed so that its characteristics replicate the real state as close as possible. Jaw model has been designed according to the real one (Fig. 2 (a)) created by the dentist prosthodontist. Generally, the dimensions of the jaw vary and depend on an individual person. In this study, the dimensions of the jaw model (Fig. 2 (b)) are adjusted for the child's head model as well as for the adult's head model. In addition, this jaw model was positioned inside child's and adult's models as shown in Fig. 2 (c).

The model of an actual smartphone has been developed as a source of electromagnetic radiation (Fig. 3). The cell phone model contains the following parts: the display, cell phone housing and planar inverted F antenna (PIFA). The PIFA, as a source of electromagnetic radiation, was modelled with the output power $P=1 \text{ W}$ [33] and the impedance $Z=50 \Omega$. The PIFA antenna consists of a radiating patch, ground plane, feed and shorting strip. The detailed description and PIFA dimensions can be found in [16]. The return loss characteristic of PIFA is shown in Fig. 3.

It should be noted that the smartphone with PIFA antenna, used in this study, is positioned in the microphone area (at the user mouth level). The mobile phone is positioned on the right side of the head model

and slanted towards the face, Fig. 4. This position of mobile phone is typical for conversation scenario.

Table 1: Electromagnetic properties of tissues and organs for an adult person

Biological Tissue		3G 0.9GHz	4G 2.6GHz	5G 28GHz	$\rho[\text{kgm}^{-3}]$	
1	Cortical Bones	ϵ_r	12.45	11.3	5.17	1908
		$\sigma [\text{Sm}^{-1}]$	0.143	0.424	4.94	
2	Brain*	ϵ_r	49.4	44.5	19.2	1046
		$\sigma [\text{Sm}^{-1}]$	1.26	2.2	27.6	
3	Cerebrospinal Fluid	ϵ_r	68.60	66	28.2	1007
		$\sigma [\text{Sm}^{-1}]$	2.410	3.6	43.8	
4	Fat	ϵ_r	11.30	10.8	6.09	911
		$\sigma [\text{Sm}^{-1}]$	0.109	0.28	5.04	
5	Cartilage	ϵ_r	42.70	38.4	13.2	1100
		$\sigma [\text{Sm}^{-1}]$	0.782	1.87	20	
6	Pituitary Gland	ϵ_r	59.70	57	24.5	1053
		$\sigma [\text{Sm}^{-1}]$	1.040	2.09	36.2	
7	Spinal Cord	ϵ_r	32.50	30	13.9	1075
		$\sigma [\text{Sm}^{-1}]$	0.574	1.15	17.6	
8	Muscle	ϵ_r	55.00	52.5	24.4	1090
		$\sigma [\text{Sm}^{-1}]$	0.943	1.84	33.6	
9	Eyes*	ϵ_r	49.60	47.55	20.15	1060
		$\sigma [\text{Sm}^{-1}]$	0.994	2.08	30.87	
10	Skin	ϵ_r	41.40	37.8	16.6	1109
		$\sigma [\text{Sm}^{-1}]$	0.867	1.54	25.8	
11	Tongue	ϵ_r	55.30	52.4	22.7	1090
		$\sigma [\text{Sm}^{-1}]$	0.936	1.92	33	
12	Teeth	ϵ_r	12.50	11.3	5.17	2180
		$\sigma [\text{Sm}^{-1}]$	0.143	0.424	4.94	

* Characteristics of tissues are defined as an average value.

In order to create numerical models with correctly associated electromagnetic properties of biological tissues and organs and determine the spatial distribution of the electromagnetic field (that originates from a cell phone) within the model, the Computer Simulation Technology (CST) software package is used. This software is based on the FIT (Finite Integration Technique) method [34]. The simulation is realized in time domain using Transient Solver included into CST package and the source is modelled as discrete port.

Before any computation it is necessary to define appropriate boundary conditions that define the electromagnetic wave propagation within the environment of the model. Open (add space) boundary conditions, that assume perfectly matched microwave absorber material at the boundary, have been applied in order to insure that the closest fields is not in the contact with the boundary, since the best results are obtained in

that way.

When using the CST software package, the key step before computation is to create the mesh of elements. A finer mesh means a greater number of elements, which makes the results more accurate. On the other hand, a finer mesh requires more powerful hardware and computational time (that can last for days for some applications). Therefore, it is essential to find the proper balance between the result accuracy and computation time. For numerical analysis presented in this paper, it was necessary to perform the test of convergence in order to demonstrate that the results do not depend on appropriate number of required mesh elements.

With mesh created in this way, for computation of electromagnetic field propagation and SAR, the computer resources with the following specifications have been used: RAM-32 GB, processor-4 core (3.20 GHz).

Table 2: Electromagnetic properties of tissues and organs for a child

Biological Tissue		3G 0.9GHz	4G 2.6GHz	5G 28GHz	ρ [kgm ⁻³]	
1	Cortical Bones	ϵ_r	14.79	13.42	6.12	1908
		σ [Sm ⁻¹]	0.180	0.53	6.21	
2	Brain*	ϵ_r	55.24	53.67	23.15	1046
		σ [Sm ⁻¹]	1.39	2.76	34.56	
3	Cerebrospinal Fluid	ϵ_r	81.84	78.74	33.64	1007
		σ [Sm ⁻¹]	2.93	4.38	53.25	
4	Fat	ϵ_r	13.48	12.88	7.26	911
		σ [Sm ⁻¹]	0.132	0.34	6.11	
5	Cartilage	ϵ_r	49.11	44.16	15.18	1100
		σ [Sm ⁻¹]	0.899	2.15	22.3	
6	Pituitary Gland	ϵ_r	62.09	59.28	25.48	1053
		σ [Sm ⁻¹]	1.082	2.17	37.65	
7	Spinal Cord	ϵ_r	38.77	35.79	16.54	1075
		σ [Sm ⁻¹]	0.697	1.39	21.296	
8	Muscle	ϵ_r	62.32	59.48	27.57	1090
		σ [Sm ⁻¹]	1.065	2.08	37.97	
9	Eyes*	ϵ_r	59.17	56.72	24.04	1060
		σ [Sm ⁻¹]	1.212	2.54	37.66	
10	Skin	ϵ_r	51.58	47.09	20.67	1109
		σ [Sm ⁻¹]	1.078	1.91	31.48	
11	Tongue	ϵ_r	55.30	52.4	22.7	1090
		σ [Sm ⁻¹]	0.936	1.92	33	
12	Teeth	ϵ_r	14.79	13.37	6.11	2180
		σ [Sm ⁻¹]	0.180	0.533	6.17	

* Characteristics of tissues are defined as an average value.

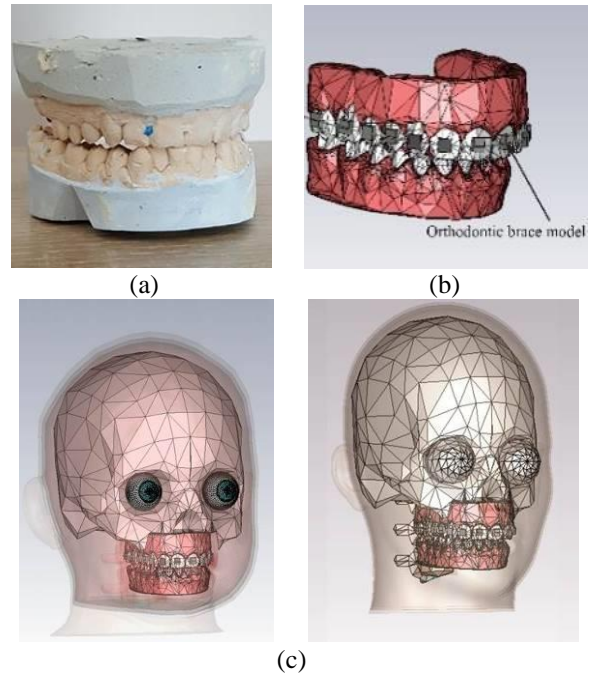


Fig. 2. External appearance of the jaw: (a) artificial human jaw created by dentist prosthetics, (b) assembled model of the jaw and orthodontic brace used for simulation, and (c) position of the assembled model inside the child's head model (left) and adult's head model (right).

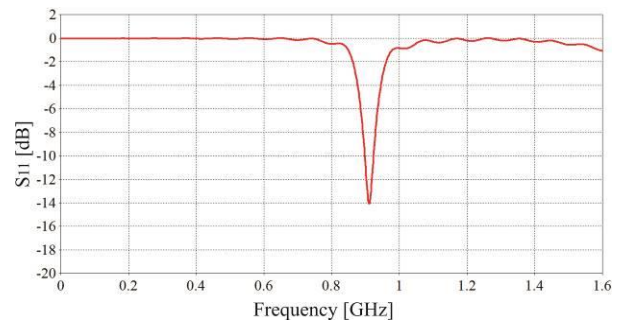


Fig. 3. Return loss of the PIFA antenna (dB).

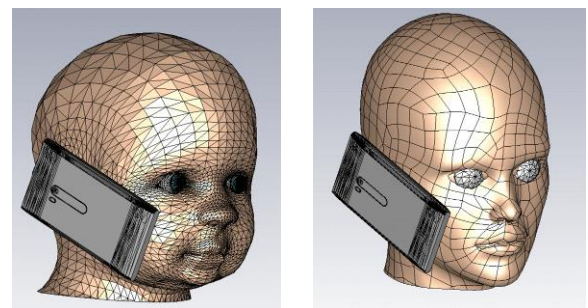


Fig. 4. The external look of the smartphone and its position.

B. SAR calculation

The SAR is a measure of the radio frequency (RF) energy rate absorbed by the body, in terms of watts per kilogram (W/kg) averaged over a small sample of tissue. SAR is defined as the speed of power dissipation normalised by the density of the material, and can be described by the following equation [35]:

$$\text{SAR} = \frac{\sigma}{\rho} |E|^2, \quad (1)$$

where σ is the electrical conductivity (S/m) and ρ is the density of tissue (kg/m^3). It should be also noted that the electric field E (V/m) is the r.m.s. value.

In addition, the averaged SAR can be defined as the ratio of the power absorbed in the tissue and the weight of that biological tissue. The averaged SAR is obtained by integrating SAR value over the observed volume:

$$\text{SAR}_{\text{av}} = \frac{1}{V} \int_V \text{SAR} dV = \frac{1}{V} \int_V \frac{\sigma}{\rho} |E|^2 dV. \quad (2)$$

Mass averaged SAR in this study is calculated for a sample of 1g ($\text{SAR}_{1\text{g}}$) and a sample of 10g ($\text{SAR}_{10\text{g}}$).

III. RESULTS

In this section, electric field and SAR distribution will be shown at the cross-sections of both models (child and adult) at the level of the orthodontic brace. Comparative analysis of the obtained results for models with and without orthodontic brace will be carried out using child head and adult head model.

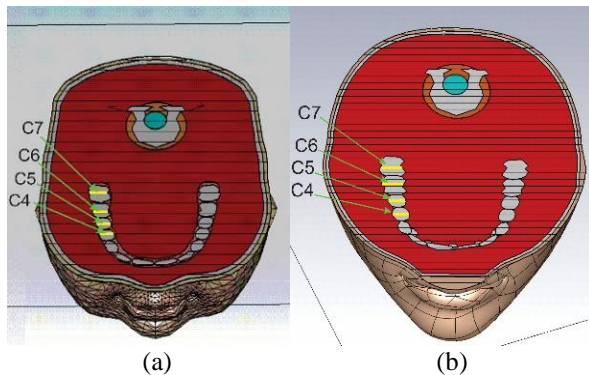


Fig. 5. Cross-section and curves for evaluating electric field and SAR distribution: (a) child and (b) adult.

The obtained results of electric field within the teeth are represented as a function of the distance from the radiation source along the curves shown in Fig. 5. Numerical labels of the curves from Fig. 5 correspond to the teeth labels (Table 3 – Table 5). The results for electric field strength and amount of absorbed energy are represented for the teeth that are on the same side as the

source of electromagnetic radiation (cell phone). These teeth are the most exposed to the electromagnetic radiation. All curves are located in the same planes with the orthodontic brace.

Also it should be noted that the maximum value of electric field as well as SAR value in the colour palette on the right side of the figures is set to be the same for both models and for all frequencies, in order to enable the easier comparison.

A. Electric field distribution

This section deals with a comparative analysis of the electric field distribution in the vicinity of the orthodontic brace, positioned in the child's and adult's model, at the frequency of 3G mobile networks.

It should be mentioned that the allowable values for the electric field are: 41 V/m at 0.9 GHz [5-8].

The spatial distribution of the electric field for the horizontal cross-section located at the mouth level, is shown in Fig. 6.

The peak of electric field strength exists in the vicinity of the orthodontic brace (Figs. 6 (b) and (d)) in the case of both models (child and adult). The obtained results for maximum values of electric field strength within certain teeth, for the models with and without the orthodontic brace, are represented in Table 3 (labels of the teeth correspond to the ones from Fig. 6).

The dependence of the electric field along the curves (Fig. 5) within the teeth, as a function of a distance from the radiation source, for the models with and without the orthodontic brace, is given in Figs. 7 and 8.

According to these figures, the differences in the values of the electric field can be noted. It is evident that the value of the electric field is significantly greater in the presence of an orthodontic brace for both models. Based on the results shown in Figs. 6-8, as well as the results given in Table 3, the overall conclusion is that the presence of an orthodontic brace increases the electric field strength within the teeth.

Also it is noticeable that the electric field strength in the case of a child is higher comparing to the adult case. This was expected due to the differences between the dielectric characteristics and also because of the differences in dimensions.

B. Specific absorption rate

This section presents the impact of orthodontic brace on the SAR values, in the case of the child's head and adult's head model. The dependence of the $\text{SAR}_{1\text{g}}$ and $\text{SAR}_{10\text{g}}$, along the curves within teeth, versus the distance from the radiation source and for different frequencies, is represented.

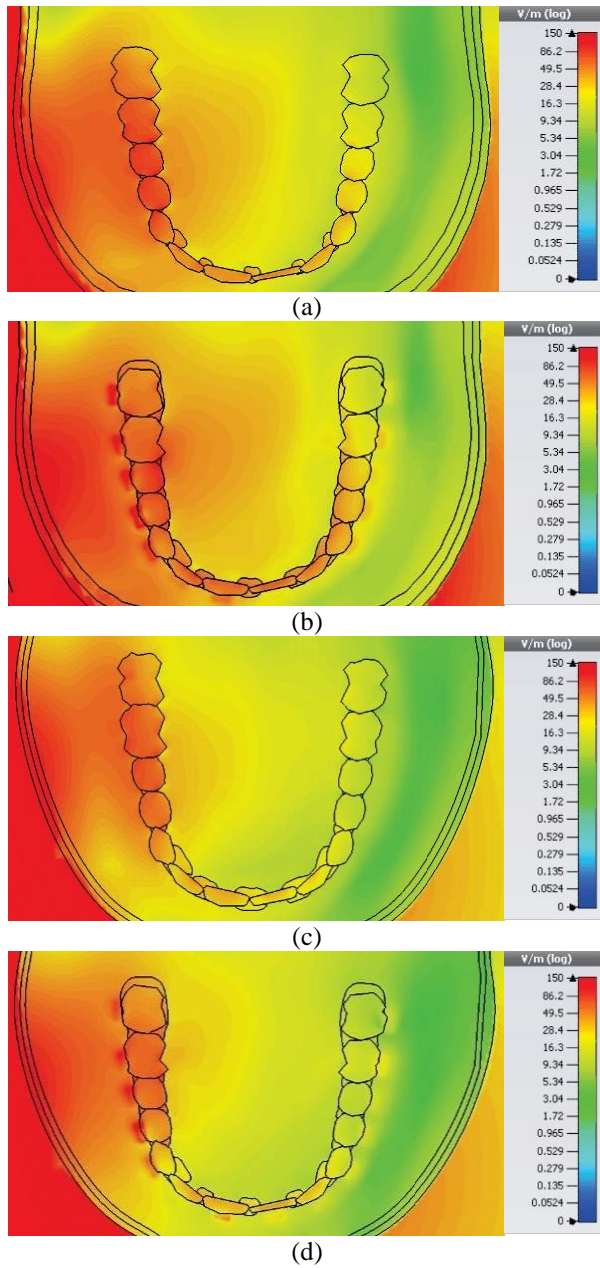


Fig. 6. Spatial distribution of electric field within the models: (a) child without orthodontic brace, (b) child with orthodontic brace, (c) adult without orthodontic brace, and (d) adult with orthodontic brace.

Table 3: Maximum value of the electric field strength within teeth - E [V/m]

Tooth	Child without Orthodontic Brace	Child with Orthodontic Brace	Adult without Orthodontic Brace	Adult with Orthodontic Brace
No. 4	79.89	128.93	52.92	115.88
No. 5	87.41	223.76	71.63	129.94
No. 6	83.25	194.52	67.54	121.62
No. 7	62.67	130.07	46.49	90.01

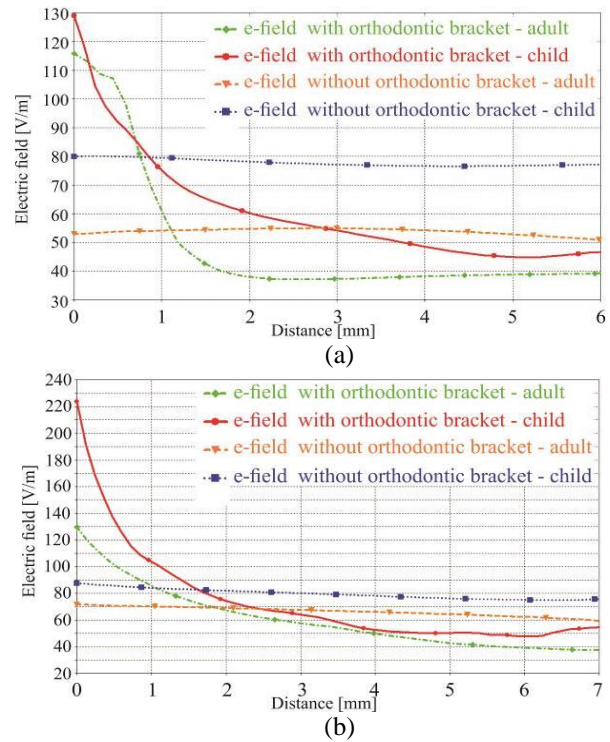


Fig. 7. Electric field strength along the curves: (a) C4 and (b) C5.

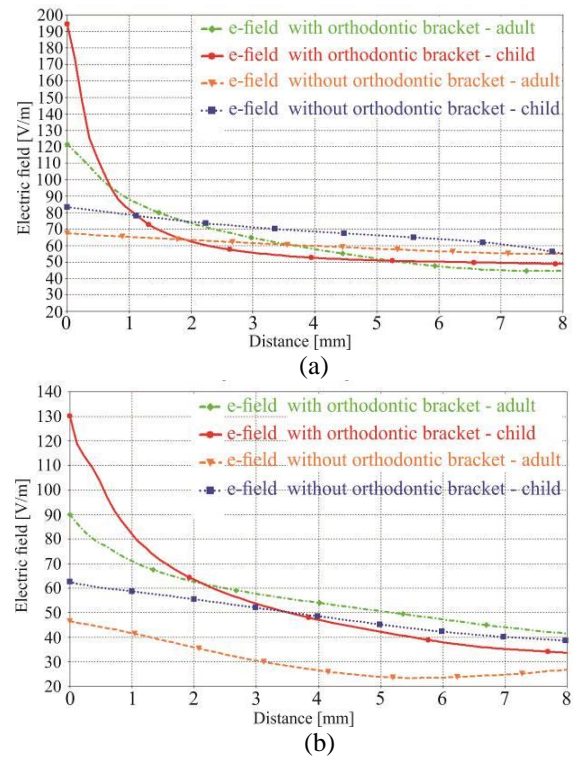


Fig. 8. Electric field strength along the curves: (a) C6 and (b) C7.

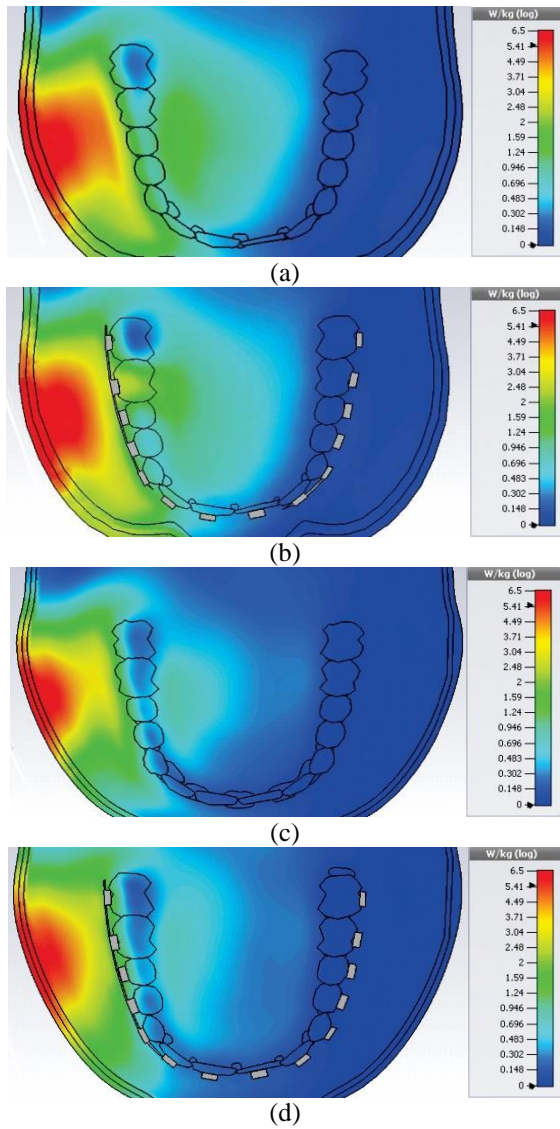


Fig. 9. Spatial distribution of SAR_{1g} : (a) child without orthodontic brace, (b) child with orthodontic brace, (c) adult without orthodontic brace, and (d) adult with orthodontic brace.

It should be mentioned that, according to appropriate safety standards, the limit of SAR for public exposure from cell phones is 1.6 watts per kilogram (1.6 W/kg) for SAR_{1g} and 2 watts per kilogram (2 W/kg) for SAR_{10g} [5].

The spatial distribution of SAR averaged for 1g (SAR_{1g}) within the models (with and without orthodontic brace) in the case of child and adult is represented in Fig. 9. The maximum value of SAR in the colour palette is set to be the same for both models.

The dependence of the SAR_{1g} and SAR_{10g} along the curves within teeth, versus the distance from the radiation source, for the model (child and adult) with and without the orthodontic brace, is given in Figs. 10-13.

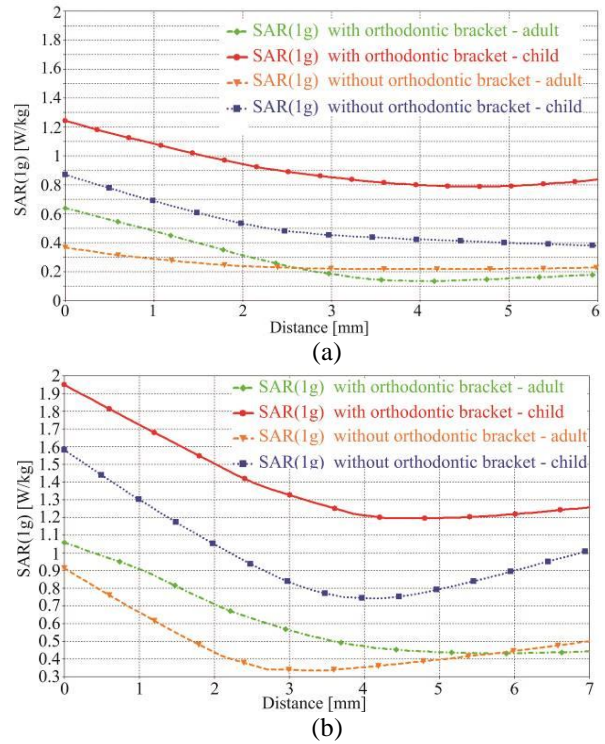


Fig. 10. Specific absorption rate - SAR_{1g} along the curves: (a) C4 and (b) C5.

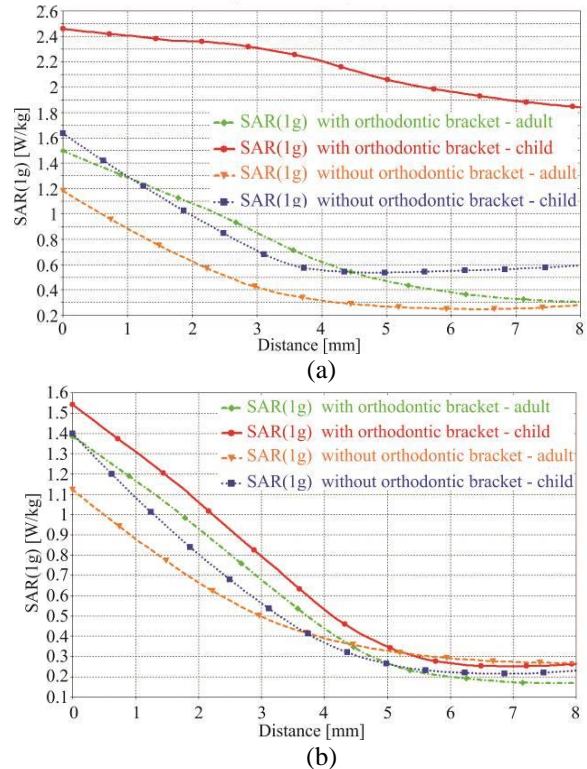


Fig. 11. Specific absorption rate - SAR_{1g} along the curves: (a) C6 and (b) C7.

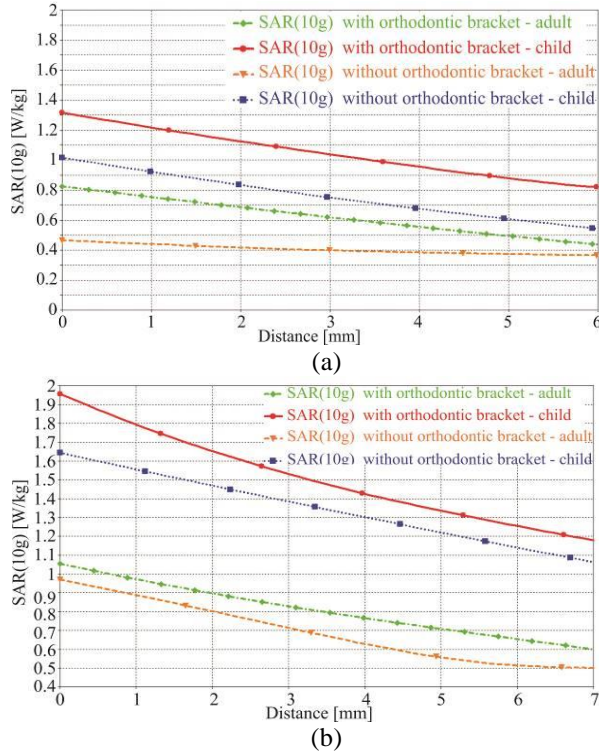


Fig. 12. Specific absorption rate - SAR_{10g} along the curves: (a) C4 and (b) C5.

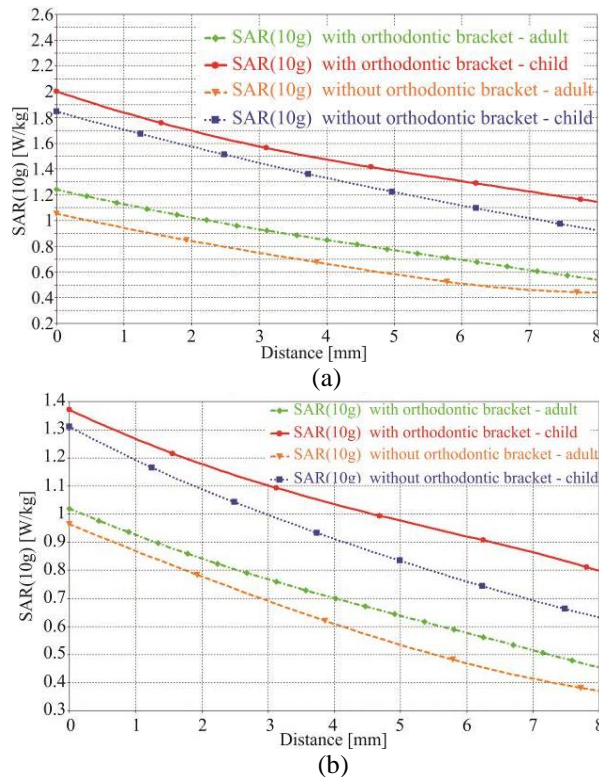


Fig. 13. Specific absorption rate - SAR_{10g} along the curves: (a) C6 and (b) C7.

The maximum values of the SAR_{1g} and SAR_{10g} within certain teeth, for the models with and without orthodontic brace, are represented in Tables 4 and 5, respectively.

Table 4: Maximum value of SAR_{1g} [W/kg]

Tooth	Child without Orthodontic Brace	Child with Orthodontic Brace	Adult without Orthodontic Brace	Adult with Orthodontic Brace
No. 4	0.88	1.27	0.37	0.64
No. 5	1.58	1.95	0.91	1.06
No. 6	1.73	2.46	1.18	1.49
No. 7	1.4	1.55	1.14	1.38

Table 5: Maximum value of SAR_{10g} [W/kg]

Tooth	Child without Orthodontic Brace	Child with Orthodontic Brace	Adult without Orthodontic Brace	Adult with Orthodontic Brace
No. 4	1.01	1.32	0.46	0.825
No. 5	1.64	1.96	0.95	1.05
No. 6	1.84	2.01	1.05	1.24
No. 7	1.21	1.37	0.96	1.02

Based on the results represented in Figs. 10-13 and results shown in Table 4 and Table 5, the increase of the SAR_{1g} and SAR_{10g} values can be noticed in the presence of the orthodontic brace. Also, it can be seen that the SAR_{1g} and SAR_{10g} values are higher in the case of child's head model.

V. DISCUSSION

According to the obtained results for the electric field distribution, in the vicinity of the orthodontic brace exposed to the cell phone radiation, the maximum value of electric field is greater in the presence of the orthodontic brace in the case of child as well as in the case of adult head model. This can be seen from Figs. 6 – 8 and Table 3.

Based on the results given in Table 3, one can see that the highest value of the electric field strength was found in the tooth No. 5. This value in the case of child is 223.76 V/m, which is about 155% higher comparing to the child model without orthodontic brace and 72% higher comparing to the adult with orthodontic brace (129.94 V/m).

The significant deviation of the electric field strength can be also noted within the tooth No. 6. Nevertheless, the impact of orthodontic brace on the electric field cannot be neglected within other teeth.

Since the referent value for the electric field, prescribed by adequate standards at 0.9 GHz, is 41 V/m, comparing the results obtained by numerical calculation with values prescribed by safety standards, it is evident that obtained results exceed the referent levels inside all teeth in both models (with and without the orthodontic brace). However, it should be kept in mind that in the case of model with orthodontic brace the values are many times greater than the allowable values.

Regarding the obtained results for SAR within the teeth, in the presence of an orthodontic brace, a significant increase in the amount of absorbed energy can be observed. The maximum of SAR_{1g} occurs in the tooth No. 6 in the case of a child (2.46W/kg). This value is about 65% higher comparing to the adult with orthodontic brace and 45% higher comparing to the results obtained for a child without orthodontic brace. In this tooth and tooth No. 5, the SAR_{1g} overcomes the safety values but only in the case of child in the presence of the orthodontic brace. The amount of absorbed energy inside the other teeth satisfies basic restriction. However, the increase in the amount of absorbed energy in the presence of an orthodontic brace is not negligible.

Based on the results, obtained for SAR_{10g} , (Table 5) it can be noticed that the SAR_{10g} overcomes the safety values but only in tooth No. 6 and only in the case of child with the orthodontic brace. Hence, the increase in the SAR_{10g} value can be noticed in the presence of the orthodontic brace.

VI. CONCLUSION

This study deals with the electric field distribution and the amount of absorbed energy within teeth, in the presence of an orthodontic brace, exposed to the electromagnetic radiation from the cell phone. The numerical calculation was performed for the frequency of 3G mobile network (0.9GHz).

The comparative analysis is presented for two models, child's head model and adult's head model.

Based on the obtained results, one can conclude that the presence of orthodontic brace causes increase of electric field and SAR within the teeth. In some cases, those values overcome referent limits for electric field strength, i.e., safety limits for SAR values. In addition, it is important to note that the obtained results are valid for investigated specific scenario, which is based on simulation model presented in this study.

Also, according to the results obtained by numerical calculation using child head model as well as adult head model, it can be concluded that certain variations in the values of electric field and SAR exist.

Because of the mentioned before and the fact that each standard contains specific safety limits of exposure to electromagnetic fields but they have been developed based on the research for adults, it should be established if they are sufficiently valid also in case of children.

The future researches should be focused on the impact of orthodontic brace on the electric field strength and amount of absorbed energy at the frequency of LTE-4G, and the latest generation of mobile networks – 5G.

The results obtained in this research can represent a good base for multidisciplinary studies involving medical professionals. It is the proper way of studying the biological effects due to the influence of orthodontic

brace presence exposed to the electromagnetic radiation from a cell phone.

ACKNOWLEDGMENT

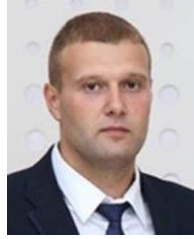
The research presented in this paper is financed by the Ministry of Education, Science and Technological Development of the Republic of Serbia under the project TR33035.

REFERENCES

- [1] W. G. Whittow, R. M. Edwards, C. J. Panagamuwa, and J. C. Vardaxoglou, "Effect of tongue jewellery and orthodontist metallic braces on the sar due to mobile phones in different anatomical human head models including children," *2008 Loughborough Antennas and Propagation Conference*, Loughborough, UK, pp. 293-296, 2008.
- [2] S. M. Mortazavi, M. Paknahad, I. Khaleghi, and M. Eghlidospour, "Effect of radiofrequency electromagnetic fields (RF-EMFS) from mobile phones on nickel release from orthodontic brackets: An in vitro study," *International orthodontics*, vol. 16, no. 2, pp. 562-570, 2018.
- [3] Y. Fujii, "Gold alloy dental inlay for preventing involuntary body movements caused by electromagnetic waves emitted by a cell phone," *Open Journal of Antennas and Propagation*, vol. 2, no. 4, pp. 37-43, 2014.
- [4] O. P. Gandhi, "Yes the children are more exposed to radiofrequency energy from mobile telephones than adults," *IEEE Access*, vol. 3, pp. 985-988, 2015.
- [5] Council of the European Union, "Council recommendation of 12 July 1999 on the limitation of exposure of the general public to electromagnetic fields (0 Hz to 300 GHz)," (1999/519/EC 1999), *Official Journal of European Communities*, L 199/59-70, 1999.
- [6] IEEE - Institute of Electrical and Electronics Engineers, "IEEE Standard for safety levels with respect to human exposure to radio frequency electromagnetic fields, 3 kHz to 300 GHz," *Inc. C95.1-2005*, 2006.
- [7] Ministarstvo prostornog planiranja i životne sredine Republike Srbije [Ministry of Spatial Planning and Environment of the Republic of Serbia], "Pravilnik o granicama izlaganja nejonizujućim zračenjima [Rulebook on limits of exposure to non-ionizing radiation]," *Službeni glasnik Republike Srbije [Official Gazette of Republic of Serbia]*, 104/09, [in Serbian], 2009.
- [8] International Commission on Non-ionizing Radiation Protection, "ICNIRP statement on the guidelines for limiting exposure to time-varying electric, magnetic, and electromagnetic fields (up

- to 300 GHz),” *Health Physics*, vol. 74, no. 4, pp. 494-522, 1998.
- [9] International Agency for Research on Cancers, “IARC classifies radiofrequency electromagnetic fields as possibly carcinogenic to humans,” *Press Release*, no. 208, 2008.
- [10] R. Hirt and G. Schmid, “Numerical analysis of specific absorption rate in the human head due to a 13.56 MHz RFID-based intra-ocular pressure measurement system,” *Physics in Medicine & Biology*, vol. 58, no. 18, pp. 267-277, 2013.
- [11] F. Schaumburg and F. A. Guarnieri, “Assessment of thermal effects in a model of the human head implanted with a wireless active microvalve for the treatment of glaucoma creating a filtering bleb,” *Physics in Medicine & Biology*, vol. 62, no. 9, pp. 191-203, 2017.
- [12] C. Buccella, V. De Santis, and M. Feliziani, “Numerical prediction of SAR and thermal elevation in a 0.25-mm 3-D model of the human eye exposed to handheld transmitters,” *IEEE International Symposium on Electromagnetic Compatibility*, Honolulu, HI, USA, pp. 1-6, 2007.
- [13] V. Stankovic, D. Jovanovic, D. Krstic, V. Markovic, and N. Cvetkovic, “Temperature distribution and specific absorption rate inside a child’s head,” *International Journal of Heat and Mass Transfer*, vol. 104, pp. 559-565, 2017.
- [14] V. Stankovic, D. Jovanovic, D. Krstic, V. Markovic, and M. Dunjic, “Calculation of electromagnetic field from mobile phone induced in the pituitary gland of children head model,” *Vojnosanitetski Pregled*, vol. 74, no. 9, pp. 854-861, 2017.
- [15] F. Kaburcuk and A. Z. Elsherbeni, “Temperature rise and SAR distribution at wide range of frequencies in a human head due to an antenna radiation,” *ACES Journal*, vol. 33, no. 4, pp. 367-372, 2018.
- [16] M. I. Hossain, M. R. I. Faruque, and M. T. Islam, “A new design of cell phone body for the SAR reduction in the human head,” *ACES Journal*, vol. 30, no. 7, pp. 792-798, 2015.
- [17] F. Kaburcuk, “Effects of a brain tumor in a dispersive human head on SAR and temperature rise distributions due to RF sources at 4G and 5G frequencies,” *Electromagnetic Biology and Medicine*, vol. 38, no. 2, pp. 168-176, 2019.
- [18] Dassault Systèmes, CST (Computer Simulation Technology) Studio Suite, 2009.
- [19] M. Martinez-Burdalo, A. Martin, M. Anguiano, and R. Villar, “Comparison of FDTD-calculated specific absorption rate in adults and children when using a mobile phone at 900 and 1800 MHz,” *Physics in Medicine and Biology*, vol. 49, pp. 345-354, 2004.
- [20] J. Keshvari and S. Lang, “Comparison of radio frequency energy absorption in ear and eye region of children and adults at 900, 1800 and 2450 MHz,” *Physics in Medicine and Biology*, vol. 50, pp. 4355-4369, 2005.
- [21] A. A. de Salles, G. Bulla, and C. E. Rodriguez, “Electromagnetic absorption in the head of adults and children due to mobile phone operation close to the head,” *Electromagnetic Biology and Medicine*, vol. 25, pp. 349-360, 2006.
- [22] J. Wiart, A. Hadjem, M. F. Wong, and I. Bloch, “Analysis of RF exposure in the head tissues of children and adults,” *Physics in Medicine and Biology*, vol. 53, pp. 3681-3695, 2008.
- [23] A. Christ, M. C. Gosselin, S. Kühn, and N. Kuster, “Impact of pinna compression on the RF absorption in the heads of adult and juvenile cell phone users,” *Bioelectromagnetics*, vol. 31, pp. 406-412, 2010.
- [24] O. P. Gandhi, L. L. Morgan, A. A. de Salles, Y. Y. Han, R. B. Herberman, and D. L. Davis, “Exposure limits: The underestimation of absorbed cell phone radiation, especially in children,” *Electromagnetic Biology and Medicine*, vol. 31, pp. 34-51, 2012.
- [25] L. L. Morgan, S. Kesari, and D. L. Davis, “Why children absorb more microwave radiation than adults: The consequences,” *Journal of Microscopy and Ultrastructure*, vol. 2, pp. 197-204, 2014.
- [26] A. Christ, M. C. Gosselin, M. Christopoulou, S. Kühnand, and N. Kuster, “Age-dependent tissue-specific exposure of cell phone users,” *Physics in Medicine and Biology*, vol. 55, pp. 1767-1783, 2010.
- [27] J. Wang, O. Fujiwara, and S. Watanabe, “Approximation of aging effect on dielectric tissue properties for SAR assessment of mobile telephones,” *IEEE Transactions on Electromagnetic Compatibility*, vol. 48, pp. 408-413, 2006.
- [28] A. Peyman, A. A. Rezazadeh, and C. Gabriel, “Changes in the dielectric properties of rat tissue as a function of age at microwave frequencies. Corrections to Peyman et al. (2001),” *Physics in Medicine and Niology*, vol. 47. pp. 2187-2188, 2002.
- [29] G. Schmid and R. Uberbacher, “Age dependence of dielectric properties of bovine brain and ocular tissue in the frequency range of 400 MHz to 18 GHz,” *Physics in Medicine and Biology*, vol. 50, pp. 4711-4720, 2005.
- [30] ITIS Foundation, Dielectric properties of tissues, Available at: <https://goo.gl/76SnEN>
- [31] C. R. Fernández, G. Bulla, A. C. Pedra, and A. A. de Salles, “Comparison of electromagnetic absorption characteristics in the head of adult and a children for 1800 MHz mobile phones,” *International Conference on Microwave and*

- Optoelectronics*, Brasilia, Brazil, pp. 523-528, 2005.
- [32] S. M. Castro, M. J. Ponces, J. D. Lopes, M. Casconcelos, and M. C. F. Pollmann, "Orthodontic wires and its corrosion—The specific case of stainless steel and beta-titanium," *Journal of Dental Sciences*, vol. 10, no. 1, pp. 1-7, 2015.
- [33] IEEE - Institute of Electrical and Electronics Engineers, "IEEE recommended practice for measurements and computations of radio frequency electromagnetic fields with respect to human exposure to such fields, 100kHz-300GHz," *Inc. C95.3-2002*, 2002.
- [34] M. Clemens and T. Weiland, "Discrete electromagnetism with the finite integration technique," *Progress in Electromagnetic Research*, vol. 32, pp. 65-87, 2001.
- [35] M. A. Ebrahimi-Ganjeh and A. R. Attari, "Interaction of dual band helical and PIFA handset antennas with human head and hand," *Progress in Electromagnetic Research*, vol. 77, pp. 225-242, 2007.



Dejan Jovanovic was born in Prokuplje, Serbia. He obtained M.Sc. degree at the Faculty of Electronic Engineering, University of Nis, Serbia in 2013. Jovanovic is a Ph.D. student at Faculty of Electronic Engineering, University of Nis. His main areas of research include numerical methods for electromagnetic field calculation and electromagnetic radiations.